Probabilistic Engineering Mechanics 81 (2025) 103792

Contents lists available at ScienceDirect

Probabilistic Engineering Mechanics

journal homepage: www.elsevier.com/locate/probengmech

A comparative analysis of intrusive and non-intrusive PCE methods for random mode computation

Eric Jacquelin [a,*], Sondipon Adhikari [b], Denis Brizard [a]

[a] Univ Lyon, Univ Gustave Eiffel, Univ Claude Bernard Lyon 1, LBMC UMR-T 9406, Lyon, F-69622, France
[b] James Watt School of Engineering, The University of Glasgow, Glasgow, UK

ARTICLE INFO

Dataset link: Random Modes (Original data)

Keywords:
Random dynamical systems
Polynomial chaos expansion
Non-intrusive approach
Intrusive approach
Random modes

ABSTRACT

Random eigenmodes present a significant challenge in the analysis of uncertain dynamical systems, particularly when traditional Monte Carlo methods become computationally prohibitive for high-dimensional problems. While Polynomial Chaos Expansion (PCE) offers a promising alternative, the choice between intrusive (physics-based) and non-intrusive (data-driven) implementations remains a critical yet understudied decision. This paper presents the first comprehensive comparison of these PCE approaches for random eigenmode computation, examining their theoretical foundations, implementation complexities, and computational efficiency. Through systematic analysis of a three-degree-of-freedom system with varying uncertainty parameters, we demonstrate that intrusive PCE achieves superior accuracy for low-dimensional problems, while non-intrusive PCE shows better scalability for higher-dimensional systems. Our findings reveal a previously undocumented trade-off between implementation complexity and computational efficiency, establishing clear criteria for approach selection based on problem dimensionality and accuracy requirements. These insights extend beyond modal analysis to the broader field of uncertainty quantification in computational mechanics, providing practical guidelines for selecting optimal PCE strategies in various engineering applications. The methodological framework presented here opens new possibilities for efficient uncertainty analysis in large-scale dynamical systems.

1. Introduction

The main objective of this work is to determine the random modes of a dynamical system whose parameters can be described by random variables. The random eigenproblem is studied non only in applied mathematics [1–3] but also in structural dynamics [4–11]. Indeed, the response of a random dynamical system can be calculated from the random eigenmodes either in the frequency domains [9] or in the time domain [12].

Direct Monte Carlo simulation (D-MCS) is the simplest method to describe a random quantity. D-MCS consists in providing samples of the eigenmodes: statistics are drawn from the samples. However, estimating the probability density function (pdf) of the eigenmodes requires a very large number of samples. The large number of simulation combined with the fact that the cost of solving an eigenproblem is $O(n^3)$ indicates that the numerical cost may be very high when the dof number if large. However, D-MCS is often considered as the reference method because the convergence is guaranteed.

An alternative to D-MCS is to identify metamodels with which it is possible to perform a very quick Monte Carlo simulation. The work by Ghanem and Spanos [13] on Polynomial chaos expansion has provided a frame to study random systems: it is based on the seminal work by Wiener [14] and PCE became very popular and has been studied extensively since. In particular, PCE was applied to solve random eigenproblems [7,15–17]. Zheng et al. [18] used an expansion similar to the PCE to solve the random eigenproblem. Zhang et al. [11] proposed to describe the random eigenmodes by a homotopy series to obtain the statistical moments. The method is intrusive and excellent results were obtained.

Several methods emerged to determine the PCE coefficients. They are mainly divided in two categories: the intrusive and the non intrusive approaches [19]. They are very different as one is close to the physics of the problem whereas the other is based on data. Therefore, it seems interesting to compare both approaches, which has rarely been done [20]. This is the objective of this study.

The paper is organized as follows. A general random dynamical system is described in section Section 2. Then the polynomial chaos expansion is presented in Section 3. Section 4 presents the random modes estimated with a PCE; Section 5 explains the intrusive approach

* Corresponding author.
E-mail address: eric.jacquelin@univ-lyon1.fr (E. Jacquelin).

https://doi.org/10.1016/j.probengmech.2025.103792
Received 5 March 2025; Received in revised form 27 May 2025; Accepted 5 June 2025
Available online 1 July 2025

whereas Section 6 presents the non-intrusive approach. A comparison between both approaches is illustrated with a random 3-degree-of-freedom (dof) systems in Section 7: two cases of uncertainties are investigated.

2. Random dynamical system

A linear random N-dof dynamical system is investigated. It is characterized by the mass, stiffness, and damping matrices ($\mathbf{M}$, $\mathbf{K}$, and $\mathbf{D}$), which depend on an r-element uncertain parameter vector, $\boldsymbol{\Xi}$. The dynamical response, $\mathbf{X}(t,\boldsymbol{\Xi}) \in \mathbf{R}^N$, is then the solution of the system

$$\widetilde{\mathbf{M}}(\boldsymbol{\Xi})\ddot{\mathbf{X}}(t,\boldsymbol{\Xi}) + \widetilde{\mathbf{D}}(\boldsymbol{\Xi})\,\dot{\mathbf{X}}(t,\boldsymbol{\Xi}) + \widetilde{\mathbf{K}}(\boldsymbol{\Xi})\,\mathbf{X}(t,\boldsymbol{\Xi}) = \mathbf{F}(t) \tag{1}$$

The uncertain matrices are written as

$$\widetilde{\mathbf{M}}(\boldsymbol{\Xi}) = \mathbf{M}_0 + \sum_{i=1}^{r} \xi_i \mathbf{M}_i = \sum_{i=0}^{r} \xi_i \mathbf{M}_i \tag{2}$$

$$\widetilde{\mathbf{K}}(\boldsymbol{\Xi}) = \mathbf{K}_0 + \sum_{i=1}^{r} \xi_i \mathbf{K}_i = \sum_{i=0}^{r} \xi_i \mathbf{K}_i \tag{3}$$

$$\widetilde{\mathbf{D}}(\boldsymbol{\Xi}) = \mathbf{D}_0 + \sum_{i=1}^{r} \xi_i \mathbf{D}_i = \sum_{i=0}^{r} \xi_i \mathbf{D}_i \tag{4}$$

where $\xi_0 = 1$ and $\xi_{i>0}$ represents the ith uncertain parameter with zero mean and is the ith element of random vector $\boldsymbol{\Xi}$. The related so-called deterministic dynamical system is characterized by the mean matrices ($\mathbf{M}_0$, $\mathbf{K}_0$, and $\mathbf{D}_0$).

3. Polynomial chaos

A polynomial chaos family, $\{\Psi_J(\Xi)\}_{J\in\mathbb{N}^r}$, is a set of multivariate polynomials that depend on a set of random variables Ξ such as

$$\Psi_J(\Xi) = \prod_{j=1}^{r} \psi_{J_j}(\xi_j) \tag{5}$$

where:

- J is a multi-index $J = (J_1, \dots, J_r)$; $|J| = \sum_{i=1}^{r} J_i$ is the degree of polynomial Ψ_J;
- $\{\psi_{J_j}(\xi_j)\}_{J_j\in\mathbb{N}}$ is a family of orthogonal polynomials with respect to a density measure $p_{\xi_j}(\xi_j)$ and defined over a domain D (e.g. see Table C.2);
- J_j is the degree of $\psi_{J_j}(\xi_j)$.

The choice of the jth family $\{\psi_{J_j}\}_J$ is related to the probability distribution of ξ_j (e.g., Legendre polynomial if ξ_j has a uniform distribution): if the random variables follow a different statistical law, different families of PC are used. In the following the polynomials are normalized with respect to their probability distribution:

$$\int_D \psi_{J_j}(\xi_j)\,\psi_{K_j}(\xi_j)\,p_{\xi_j}(\xi_j)\,\mathrm{d}\xi_j = \delta_{J_j,K_j} \tag{6}$$

The polynomial chaos expansion (PCE) of a random variable $\mathbf{x}(t,\Xi)$ is:

$$\mathbf{x}(t,\Xi) = \sum_{J\in\mathbb{N}^r} \mathbf{Y}_J(t)\Psi_J(\Xi) \tag{7}$$

where t represents the time. A similar expansion can be done for a frequency-dependent variable. In practice, the expansion is truncated so that the sum of the elements of J is less or equal to a fixed polynomial degree d, which is called the PCE degree.

$$\mathbf{x}(t,\Xi) \simeq \mathbf{x}^d(t,\Xi) = \sum_{\substack{J\in\mathbb{N}^r \\ |J|\le d}}^{r} \mathbf{Y}_J(t)\Psi_J(\Xi) \tag{8}$$

In the following, d is dropped to simplify the notations.

An alternative of the previous notation is [21]

$$\mathbf{x}(t,\Xi) = \sum_{p=0}^{P} \mathbf{Y}_p(t)\Psi_p(\Xi) \tag{9}$$

where $P+1$ is the PCE total number of terms. An usual rule is that if $p < q$, then the degree of $\Psi_p(\Xi)$ is lower or equal to the degree of $\Psi_q(\Xi)$ and the truncation is such that all the polynomials whose degree is lower or equal to the maximal degree are included in the expansion.

According to the rule, when Hermite and Legendre polynomials are involved, the PC of degree 0 and 1 are:

$$\Psi_0(\Xi) = 1 \tag{10}$$

$$\forall i \in \{1,\dots,r\},\quad \Psi_i(\Xi) = C_{1i} \times \xi_i \tag{11}$$

Constant C_{1i} can be found in C.2.

One notation may be preferred to the other one, depending on the context.

4. Response of a dynamical system with random modes

A natural way to obtain the response of a deterministic N-dof linear dynamical system is to expand the solution on the eigenvectors

$$\mathbf{X}(t) = \sum_{k=1}^{N} q_k(t)\,\boldsymbol{\phi}^k \tag{12}$$

where $\boldsymbol{\phi}^k$ is a deterministic eigenvector and q_k defines the deterministic modal coordinate for the kth eigenvector.

The mass and stiffness matrices are random so the eigenmodes, denoted as $\{\widetilde{\omega}_k,\ \widetilde{\boldsymbol{\phi}}^k\}$, are random as well. The random eigenproblem is formulated as

$$\left(\widetilde{\mathbf{K}} - \widetilde{\omega}_k^2\,\widetilde{\mathbf{M}}\right)\widetilde{\boldsymbol{\phi}}^k = 0 \tag{13}$$

It means that each realization of the stiffness and mass matrices gives a realization of the random modes.

The random eigenmodes can be determined with a Monte Carlo simulation (MCS) from a large number of realizations of mass and stiffness matrices: statistics may be evaluated from the random mode samples. They can also be determined with a surrogate model such as a PCE, from which it is very quick to obtain a large number of random mode samples.

The frequency response function (FRF) of the system, $\widetilde{H}(\omega)$, can be determined from the random modes

$$\widetilde{H}(\omega) = \frac{[\widetilde{\boldsymbol{\phi}}]^T[\widetilde{\boldsymbol{\phi}}]}{\widetilde{m}_n(-\omega^2 + 2\widetilde{\eta}_n\,\widetilde{\omega}_n\omega + \widetilde{\omega}_n^2)} \tag{14}$$

where $\widetilde{\eta}_n$ (resp. $\widetilde{m}_n$) is the damping ratio (resp. the generalized modal mass) of mode n.

5. Random modes: intrusive PCE approach

The random modes can be expanded as follows [4,22]

$$\widetilde{\omega}_k^2(\boldsymbol{\Xi}) = \omega_k^2 \left(\sum_{p=0}^{P} a_p^k\,\Psi_p(\boldsymbol{\Xi})\right) \tag{15}$$

$$\widetilde{\boldsymbol{\phi}}^k(\boldsymbol{\Xi}) = \sum_{n=1}^{N} \widetilde{Y}_n^k\,\boldsymbol{\phi}^n = \sum_{n=1}^{N}\left(\sum_{p=0}^{P} Y_{pn}^k\,\Psi_p(\boldsymbol{\Xi})\right)\boldsymbol{\phi}^n \tag{16}$$

where $(\omega_n,\ \boldsymbol{\phi}^n)$ denotes the n-eigenmode of the deterministic system, defined in Section 2.

$\{a_p^k,\ \{Y_{pn}^k\}_{n=1\cdots N}\}_{p=0\cdots P}$ are the PC coefficients related to the PCE of random mode k.

Further the following mass normalization is applied

$${}^T\boldsymbol{\phi}^{k\,T}\,\mathbf{M}_0\,\widetilde{\boldsymbol{\phi}}^k = 1 \tag{17}$$

where $\mathbf{M}_0$ is the mean mass matrix and ${}^T\bullet$ stands for the transpose matrix. As a consequence

$$\widetilde{Y}_k^k = 1 \tag{18}$$

Then Eq. (16) becomes

$$\widetilde{\boldsymbol{\phi}}^k = \boldsymbol{\phi}^k + \sum_{\substack{n=1\\n\neq k}}^{N}\sum_{p=0}^{P} Y_{pn}^k \, \Psi_p(\Xi)\, \boldsymbol{\phi}^n \tag{19}$$

Eqs. (15) and (19) show that the PCE of random mode k requires $N\times(P+1)$ unknowns. Projecting the eigenproblem (13) on each deterministic eigenmode $\{\boldsymbol{\phi}_n^k\}_{n=1\cdots N}$ and each PC $\{\Psi_p(\Xi)\}_{p=0\cdots P}$ gives the $N\times(P+1)$ equations.

Substituting Eqs. (2), (3), (15), (19) in Eq. (13) relates all the unknown coefficients of eigenmode k

$$\left((\sum_{i=0}^{r}\xi_i\mathbf{K}_i) - (\omega_k^2\,(\sum_{p=0}^{P}a_p^k\,\Psi_p(\Xi)))\,(\sum_{i=0}^{r}\xi_i\mathbf{M}_i)\right) \times\left(\boldsymbol{\phi}^k + \sum_{\substack{n=1\\n\neq k}}^{N}\sum_{p=0}^{P} Y_{pn}^k\,\Psi_p(\Xi)\,\boldsymbol{\phi}^n\right) = 0 \tag{20}$$

Expanding the product gives

$$\begin{aligned}&\sum_{i=0}^{r}\xi_i\mathbf{K}_i\boldsymbol{\phi}^k + \sum_{i=0}^{r}\sum_{\substack{n=1\\n\neq k}}^{N}\sum_{p=0}^{P} Y_{pn}^k\,\xi_i\Psi_p(\Xi)\,\mathbf{K}_i\boldsymbol{\phi}^n\\ &\qquad -\omega_k^2\sum_{i=0}^{r}\sum_{p=0}^{P}a_p^k\,\xi_i\Psi_p(\Xi)\,\mathbf{M}_i\boldsymbol{\phi}^k\\ -\omega_k^2\sum_{i=0}^{r}\sum_{\substack{n=1\\n\neq k}}^{N}\sum_{p=0}^{P}\sum_{q=0}^{P}&a_p^kY_{qn}^k\,\xi_i\Psi_p(\Xi)\Psi_q(\Xi)\mathbf{M}_i\boldsymbol{\phi}^n = 0\end{aligned} \tag{21}$$

Projecting Eq. (21) on each deterministic eigenvector $\boldsymbol{\phi}^l$ (l from 1 to N) and each PC $\Psi_m(\Xi)$ (m from 0 to P) gives the $N\times(P+1)$ equations of the nonlinear system to be solved to obtain the $N\times(P+1)$ PCE coefficients (i.e. a_p^k and Y_{pn}^k) of random mode k. The main difficulty is projecting on a PC when several PCs are involved. As a PC is a product of univariate polynomials, the projection on $\Psi_{J''}(\Xi)$ (multi-index notation) is a product of factors involving each univariate polynomial ψ_{J_i}. Therefore, the following expectations must be calculated:

$$<\psi_{J_i''}(\xi_i)> = <J_i''> \tag{22}$$

$$<\psi_{J_i}(\xi_i)\,\psi_{J_i''}(\xi_i)> = <J_i\;J_i''> \tag{23}$$

$$<\psi_{J_i}(\xi_i)\,\psi_{J_i'}(\xi_i)\,\psi_{J_i''}(\xi_i)> = <J_i\;J_i'\;J_i''> \tag{24}$$

$$<\xi_i\,\psi_{J_i''}(\xi_i)> = <\xi_i\;J_i''> \tag{25}$$

$$<\xi_i\,\psi_{J_i}(\xi_i)\,\psi_{J_i''}(\xi_i)> = <\xi_i\;J_i\;J_i''> \tag{26}$$

$$<\xi_i\,\psi_{J_i}(\xi_i)\,\psi_{J_i'}(\xi_i)\,\psi_{J_i''}(\xi_i)> = <\xi_i\;J_i\;J_i'\;J_i''> \tag{27}$$

where $<\bullet>=\int_D \bullet\, p_\xi(\xi)d\xi$, $p_\xi(\xi)$ is the probability density function related to ξ and D is the domain of ξ; $\psi_{J_i^\sharp}(\xi_i)$ is replaced by $J_i^\sharp$ in the scalar products, to simplify the notation as done in Eqs. (22)–(27).

More details are given in Appendix B.

A recurrence relation exists for orthogonal polynomial

$$\forall n>0,\quad \psi_{n+1}(\xi) = (a_n\,\xi - b_n)\psi_n(\xi) + c_n\psi_{n-1}(\xi) \tag{28}$$

Therefore, calculating the expectations in Eqs. (25)–(27) can be done from the expectations given in Eqs. (22)–(24). The first two expectations are calculated easily from the orthogonality properties. For Hermite and Legendre polynomials, an analytic expression of expectation (24) exists. For these polynomials the recurrence relation is simpler

$$\psi_{n+1}(\xi) = a_n\,\xi\,\psi_n(\xi) + c_n\psi_{n-1}(\xi) \tag{29}$$

6. Random modes: non-intrusive PCE approach

The same kind expansion of the random modes made in the previous Section 5 is still used:

$$\widetilde{\omega}_k^2(\Xi) = \left(\sum_{p=0}^{P} b_p^k\,\Psi_p(\Xi)\right) \tag{30}$$

$$\widetilde{\boldsymbol{\phi}}^k = \sum_{n=1}^{N}\left(\sum_{p=0}^{P} Y_{pn}^k\,\Psi_p(\Xi)\right)\boldsymbol{V}_n^k \tag{31}$$

where $\Psi_p(\Xi)$ is the pth polynomial chaos. However, $\boldsymbol{V}_n^k$ is now only the nth vector of a specific basis that may depend on the random mode, that is on k. The following bases can be used:

- the canonical basis $[\boldsymbol{V}_n^k] = [\boldsymbol{V}_n] = I_N$, where I_N is the identity matrix of size N;
- the deterministic modal basis: $[\boldsymbol{V}_n^k] = [\boldsymbol{V}_n] = [\boldsymbol{\phi}^n]$. It is the basis used in the intrusive approach;
- the proper orthogonal decomposition (POD) modes: for random mode k, the basis is derived from a sample of N_{spl} realizations of random modes k. As a consequence, the basis depends on k: $[\boldsymbol{V}_n^k] = [\boldsymbol{V}_n^{POD,k}]$.

Eq. (31) can be transformed

$$\begin{aligned}\widetilde{\boldsymbol{\phi}}^k(\Xi) &= \sum_{n=1}^{N}\left(\sum_{p=0}^{P} Y_{pn}^k\,\Psi_p(\Xi)\right)\boldsymbol{V}_n^k\\ &= \sum_{p=0}^{P}\Psi_p(\Xi)\left(\sum_{n=1}^{N}\boldsymbol{V}_n^k\,Y_{pn}^k\right)\\ &= \left(\underbrace{[\Psi_0(\Xi)\cdots\Psi_P(\Xi)]}_{{}^T[\Psi(\Xi)]}\otimes\underbrace{[\boldsymbol{V}_1^k\cdots\boldsymbol{V}_N^k]}_{[\boldsymbol{V}^k]}\right)\begin{bmatrix}Y_{01}^k\\ \cdots\\ Y_{0N}^k\\ Y_{11}^k\\ \cdots\\ Y_{PN}^k\end{bmatrix}\\ &= \left({}^T[\Psi(\Xi)]\otimes[\boldsymbol{V}^k]\right)\,[Y^k]\end{aligned} \tag{32}$$

Vector $[Y^k]$ can be determined in a non-intrusive way from N_{spl} samples $\{\widetilde{\boldsymbol{\phi}}^k(\Xi_1)\cdots\widetilde{\boldsymbol{\phi}}^k(\Xi_{\mathbf{N_{spl}}})\}$ of the random eigenvectors. The solution is obtained by regression [23] by solving the following problem:

$$\begin{aligned}\begin{bmatrix}\widetilde{\boldsymbol{\phi}}^k(\Xi_1)\\ \cdots\\ \widetilde{\boldsymbol{\phi}}^k(\Xi_{\mathbf{N_{spl}}})\end{bmatrix} &= \left(\begin{bmatrix}[\Psi(\Xi_1)]\otimes[\boldsymbol{V}^k]\\ \vdots\\ \left[\Psi(\Xi_{N_{spl}})\right]\otimes[\boldsymbol{V}^k]\end{bmatrix}\right)[Y^k]\\ &= \left(\begin{bmatrix}[{}^T\Psi(\Xi_1)]\\ \vdots\\ \left[{}^T\Psi(\Xi_{N_{spl}})\right]\end{bmatrix}\otimes[\boldsymbol{V}^k]\right)[Y^k]\end{aligned} \tag{33}$$

Problem (33) has (NN_{spl}) equations and $N(P+1)$ unknowns.

Instead of solving globally system (33), it is possible to work directly on the elements of the eigenvectors. Indeed, the coordinates of each random vector can be expressed in basis $\boldsymbol{V}^k$:

$$\widetilde{\boldsymbol{\phi}}^k(\Xi) = \sum_{n=1}^{N} c_n^k(\Xi)\,\boldsymbol{V}_n^k \tag{34}$$

Eq. (31) gives the expansion in PC of each coordinate:

$$\begin{aligned}c_n^k(\Xi) &= \sum_{p=0}^{P} Y_{pn}^k\,\Psi_p(\Xi) = [\Psi_1(\Xi)\cdots\Psi_P(\Xi)]\begin{bmatrix}Y_{0n}^k\\ Y_{1n}^k\\ \cdots\\ Y_{Pn}^k\end{bmatrix}\\ &= {}^T[\Psi(\Xi)]\begin{bmatrix}Y_{0n}^k\\ Y_{1n}^k\\ \cdots\\ Y_{Pn}^k\end{bmatrix}\end{aligned} \tag{35}$$

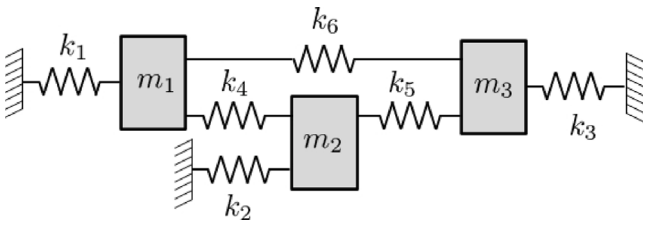

Fig. 1. 3-dof system with random coefficients.

It is also possible to identify directly each coordinate (35) of each eigenvector:

$$\begin{bmatrix} c_n^k(\Xi_1) \\ \cdots \\ c_n^k(\Xi_{\mathbf{N_{spl}}}) \end{bmatrix} = \begin{bmatrix} {}^T[\Psi(\Xi_1)] \\ \vdots \\ {}^T\left[\Psi(\Xi_{N_{spl}})\right] \end{bmatrix} \begin{bmatrix} Y_{0n}^k \\ Y_{1n}^k \\ \cdots \\ Y_{Pn}^k \end{bmatrix} \tag{36}$$

Problem (36) has N_{spl} equations and $(P+1)$ unknowns. Therefore, it has N times less equations than problem (33), but this problem must be solved N times. It seems interesting to solve both problems to assess not only the accuracy of the prediction, but also the CPU time to solve both problems.

$c_n^k(\Xi_j)$ can be obtained as follows:

- $\boldsymbol{V}^k$ is the canonical basis

$$c_n^k(\Xi_j) = \widetilde{\boldsymbol{\phi}}_n^k(\Xi_j)$$

- $\boldsymbol{V}^k$ is the deterministic modal basis

$$c_n^k(\Xi_j) = \frac{{}^T\boldsymbol{\phi}^n \, \boldsymbol{M}_{det} \, \widetilde{\boldsymbol{\phi}}^k(\Xi_j)}{\boldsymbol{M}_{mod\ n}}$$

- $\boldsymbol{V}^k$ is the POD modes

$$c_n^k(\Xi_j) = {}^T\boldsymbol{V}_n^{POD,k} \ \widetilde{\boldsymbol{\phi}}^k(\Xi_j)$$

It is possible to identify the elements of $[Y^k]$ with $N_{spl} < (P+1)N$, considering a sparse PCE: the LARS method is used in [24] and the automatic relevance determination (ARD) coupled to the variational Bayesian method (VBA), ARD-VBA, is considered in [25]: the latter method was used in this paper.

Determining the random eigenmodes with a non intrusive methods rely on N_{spl} samples of the random modes, which are calculated with a MCS. However, it is impossible to guess the right number N_{spl}. Therefore, an adaptive procedure is required to increase both the number of samples and the PCE degree until meeting a criterion, which may be a leave-one-out (LOO) error [24,25].

It is also required to split the samples in two sets: the sample used to identified the PCE coefficients (N_{id}) and the ones used to assess the quality of the PCE to predict the results (N_{val}): a relative error between the MCS and PCE results is calculated and must be below a threshold to validate the PCE.

7. Three degree-of-freedom system with several uncertain parameters

The 3-dof system shown in Fig. 1 and already used in [10] is studied. The 3 masses and the 6 stiffnesses are random:

$$\forall i \in \{1,2,3\},\ m_i = \overline{m}_i\ (1+\delta_M\ \xi_i) \tag{37}$$

$$\forall i \in \{1,\ldots,6\},\ k_i = \overline{k}_i\ (1+\delta_K\ \xi_{i+3}) \tag{38}$$

where the ξ_i are 9 standard random variables (see Table 1).

The deterministic eigenmodes are

$$\omega_1 = 1 \text{ rad/s},\ \boldsymbol{\phi}^1 = \begin{bmatrix} 1 \\ 1 \\ 1 \end{bmatrix} \omega_2 = 2 \text{ rad/s},\ \boldsymbol{\phi}^2 = \begin{bmatrix} 1 \\ -2 \\ 1 \end{bmatrix}$$

$$\omega_3 = 3 \text{ rad/s}\ \ \boldsymbol{\phi}^3 = \begin{bmatrix} 1 \\ 0 \\ -1 \end{bmatrix} \tag{39}$$

The deterministic modes are normalized such as the first element of each vector equals 1. For comparison purposes, the random mode samples will be normalized in the same way.

The direct Monte Carlo method was applied for 10 000 samples. The samples of the eigenmodes and the FRF were calculated. It was then possible to have an estimation of the statistics of the output data.

I-PCE and NI-PCE metamodels of the random eigenmodes and the random FRF were also calculated for the two approaches for several degrees and, for the non-intrusive approach, several numbers of samples used to identified NI-PCE. A MCS was carried out with the PCE metamodels for the same N_{spl}=10 000 samples used with the direct MCS. Therefore, it was possible to calculate for each sample the error based on Frobenius norm ($\|\bullet\|_F$) between the reference method (MCS or exact solution) and the PCE estimation for all the output data:

$$\mathcal{E}_{\text{data}} = \frac{\|\text{data}^{Ref} - \text{data}^{PCE}\|_F}{\|\text{data}^{Ref}\|_F} \tag{40}$$

The error will be calculated for the eigenfrequencies, the eigenvectors, but also for the FRF to have a quantity that depends on all the eigenmodes. FRFs are calculated for $n_f = 100$ frequency values in the frequency range [0 5] rad/s: $\mathcal{E}_{\text{data}}$ is calculated over the N_{spl} samples and over the n_f frequency values.

In the following two cases are addressed depending on the uncertain parameter number.

7.1. Case 1: 2 uncertain parameters

The random masses are described by one uncertain parameter ξ_1 ($\xi_1 = \xi_2 = \xi_3$), and the random stiffnesses by another uncertain parameter, ξ_4 ($\xi_4 = \xi_5 = \xi_6 = \xi_7 = \xi_8 = \xi_9$):

$$\forall i \in \{1,\ldots,3\},\quad m_i = \overline{m}_i(1+\delta_M\ \xi_1)$$
$$\forall i \in \{1,\ldots,6\},\quad k_i = \overline{k}_i(1+\delta_K\ \xi_4)$$

with ξ_1 and ξ_4 are uniform independent random variables over the interval $[-1,\ 1]$.

It means that the random matrices are proportional to the mean matrices:

$$\widetilde{\mathbf{M}}(\Xi) = (1+\delta_M\ \xi_1)\ \mathbf{M}_0$$
$$\widetilde{\mathbf{K}}(\Xi) = (1+\delta_K\ \xi_4)\ \mathbf{K}_0$$

The random modes have an analytical solution

$$\widetilde{\boldsymbol{\phi}}^k = \boldsymbol{\phi}^k \tag{41}$$

$$\widetilde{\omega}_k^2 = \omega_k^2\ \frac{1+\delta_K\ \xi_4}{1+\delta_M\ \xi_1} \tag{42}$$

It turns out that both PCE approaches are able to identify the exact random eigenvectors, that are equal to the deterministic eigenvectors. However, it is not possible to obtain the exact random squared eigenfrequencies as they are rational functions.

The error for the squared eigenfrequencies is calculated between 10 000 samples evaluated with the exact solution and the estimation obtained by the PCE metamodels. Several PCE metamodels were obtained depending on the PCE degree and also on the number of samples used to identify the PCE for NI-PCE metamodel, N_{spl}. The results are plotted in Fig. 2: the dashed black line gives the results for I-PCE approach, and the coloured lines for NI-PCE approach, for N_{spl} equals to 20, 50, 100, 200, 1000; the error on the eigenfrequencies is the same

Table 1
3-dof system characteristics.

$\overline{k}_{i=1,\dots,5}$ (Nm^{-1})	$\overline{k}_6$ (Nm^{-1})	$\overline{m}_{i=1,2,3}$ (kg)	δ_K (%)	δ_M (%)
1	3.5	1	15	15

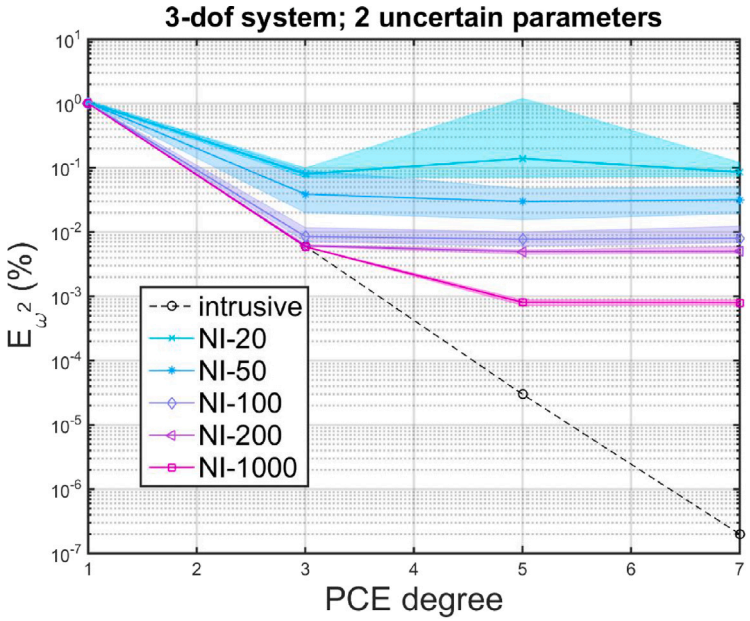

Fig. 2. 3-dof system with 2 random parameters: $\mathcal{E}_{\omega^2}$ comparison - dashed black line: I-PCE; solid coloured lines with markers: mean of sparse NI-PCE errors; coloured area: envelope of NI-PCE errors.

whatever the mode. In addition, to study the influence of the sample set, for each N_{spl} and for each PC degree, NI-PCE was identified with 20 different sets to see the robustness of the identification process. In Fig. 2, the coloured area delimits the minimum and the maximum of the 20 errors obtained with 20 NI-PCE, while the solid coloured line with the markers represents the mean error over the 20 repetitions: the larger the area, the more critical the choice of sample set.

Fig. 2 shows that the error depends on the PCE degree for I-PCE: the error decreases quickly when the degree increases.

First, for NI-PCE the influence of N_{spl} on accuracy is noticeable: by increasing the number of samples from 20 to 1000, the error is divided by 100. Second, the error is not monotonic with the PCE degree: it seems that up to N_{spl}=200, a PCE of degree greater than 3 does not give better results than a PCE of degree 3. This is common when a sparse PCE is identified: it exists an optimal PCE degree. However, if the number of samples is increased a lot (N_{spl} = 1000), the error is decreased by using a PCE of degree 5. Third, the influence of the sample set is strong when N_{spl}=20 is used, as shown by a quite large coloured area; however, the area decreases when N_{spl} increases and is almost reduced to the mean line when N_{spl} is greater or equal to 200. This highlights that the uncertain parameter space must be described by the samples well. This means that a minimum number of samples is required not only for the accuracy but also for the robustness of the identification process.

The approximation given by the sparse NI-PCE is excellent even with a PCE degree equal to one. This is confirmed by Fig. 3 where the pdfs (PCE degree equals to 3; N_{spl} = 200) of the eigenfrequencies were plotted: in both PCE approaches, the curves are very close to the one obtained from the MCS.

The same simulations were done by using an ordinary least square (OLS) regression. Usually, the results lead to an overfitting and then to poor results. In that very specific case, it turns out that the results are better than the ones obtain with a sparse NI-PCE, as shown in Fig. 4. In fact, when N_{spl} is greater than 50, the number of samples is greater than the number of coefficients even for a PCE degree equal to 7 (36 coefficients), which explains the results even if it is usually recommended to have a number of samples greater than twice the number of unknowns. In that case, the results tends to the results obtained with the I-PCE. I can also be seen that, as already mentioned, the coloured area becomes smaller when the number of samples increases.

As the statistical law is uniform, from Eq. (42), the exact mean square eigenfrequencies can be calculated:

$$\forall i \in \{1,2,3\}, \quad \bar{\omega}_i^2 = \omega_i^2 \frac{1}{2\delta_M} \log\left(\frac{1+\delta_M}{1-\delta_M}\right) \simeq 1.0076\,\omega_i^2 \tag{43}$$

Both approaches give the mean square eigenfrequency exact values.

7.2. Case 2: 9 uncertain parameters

The uncertain stiffnesses and masses depend on 9 independent random variables

$$\forall i \in \{1,\dots,3\}, \quad m_i = m_0(1+\delta_m\ \xi_i) \tag{44}$$

$$\forall i \in \{1,\dots,6\}, \quad k_i = k_0(1+\delta_k\ \xi_{i+3}) \tag{45}$$

with δ_m = 15% and δ_k = 15%. The ξ_i are 9 independent standard normal random variables. In that case, no simple analytic solution exists for the random eigenmodes.

This case highlights the limitation of the intrusive method when the random parameter number increases. Indeed, it appears on Figs. 5–6–7–8 that the results are calculated up to a PCE degree equal to 3 for the intrusive method, whereas they are calculated up to a PCE degree equal to 7 for the non-intrusive method. The reason is that most of the computing time of I-PCE is devoted to calculate the expectations given in Eqs. (22)–(27) and then to fill 2-index, 3-index and 4-index matrices (matrices $\mathbf{M3}^i$ and $\mathbf{M4}^{im}$ given in Appendix B). If the first index varies from 0 to the uncertain parameter number, the other three indices varies from 1 to the number of terms of the PCE. Therefore, the CPU simulation time (CPU-ST) may be quickly unaffordable either for

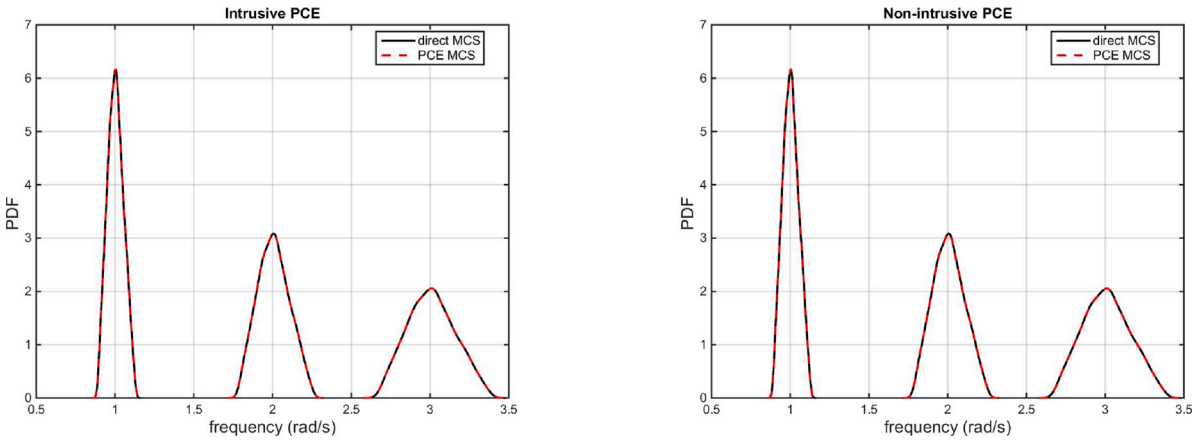

Fig. 3. Case 1: estimation of the Probability density function of the eigenfrequencies: MCS (solid black line) versus intrusive and non-intrusive PCE (dashed red line) for 2 uncertain parameters.

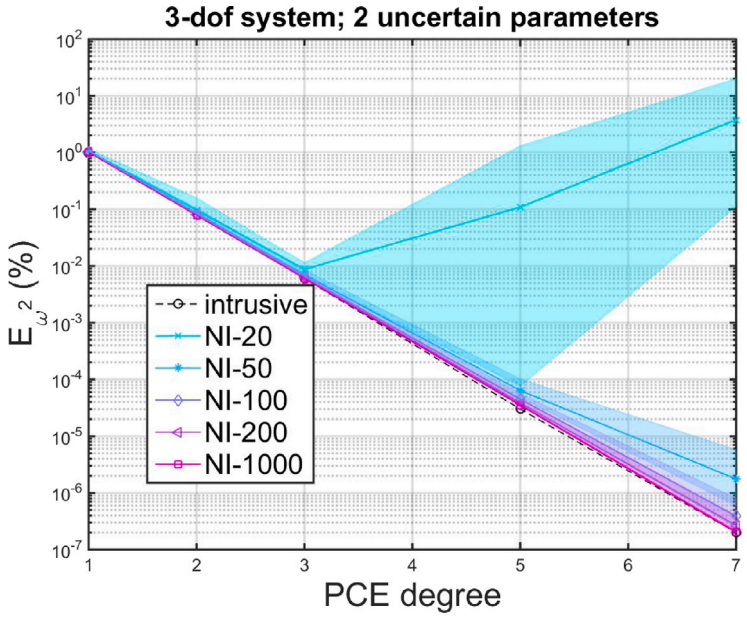

Fig. 4. 3-dof system with 2 random parameters: $\mathcal{E}_{\omega^2}$ comparison - dashed black line: I-PCE; solid coloured lines with markers: mean of OLS-PCE errors; coloured area: envelope of NI-PCE errors.

a high degree, or for a not too high number of uncertain parameters. Fig. 5 shows that the intrusive method CPU simulation time (CPU-ST) ratio (that is divided by the MCS CPU-ST) increases tremendously with the PC order and is much higher than the CPU-ST of the non-intrusive method, for the same PCE-degree.

However, the expectation matrices are not dependent on the dynamical system: they only depend on the number of PCE terms and on the distribution law. They can therefore be calculated once and stored. For example, if δ_m and δ_k are changed, the expectation matrices can be called and the CPU-ST for I-PCE would be much shorter.

I-PCE CPU-ST does not really depend on the dof number as the eigenproblem is solved once. On the contrary, the eigenproblems must be solved several times for NI-PCE. As a consequence, NI-PCE CPU-ST depends on the dof number. It also depends on the number of terms, which influences the size of the regression problem required to identify the sparse-PCE coefficients. Obviously the MCS CPU-ST depends mainly on the dof number because the eigenproblems have to be solved many times. In the example, the dynamical system has only 3 dof. Accordingly, the computation time required to solve one eigenproblem is very short: the MCS method is by far the most efficient, which explains why the CPU-ST ratio depicted in Fig. 5 is greater than 1.

Contrary to the previous case, the errors on the eigenmodes depends on the mode number. Fig. 6 shows that for the non-intrusive approach, the mean of $\mathcal{E}_{\omega^2}$ does not vary much from a PCE degree equal to 3 for a given N_{spl}, except when N_{spl}=1000 for ω_3^2. Once again, it reflects the sparsity of NI-PCE and the optimal PCE degree seems to be equal to 3 when N_{spl} is lower than 200, and 5 when N_{spl}=1000 for ω_3^2. N_{spl} must be greater than 100 to obtain errors in mean lower than 1% for all the eigenfrequencies. The intrusive method with a PCE degree of 3 gives almost always the minimal error: to obtain a slightly better error for the third eigenfrequency, N_{spl} must be equal to 1000. Increasing N_{spl} decreases the mean error. However, the intersections between coloured areas indicate that, for a given degree, the better results are not always obtained with the largest N_{spl}: this shows the strong influence of the sample set quality on the result accuracy. Contrary to case 1, even with N_{spl}=1000, the coloured area bounds are not close to the mean. In particular, even if with some sample set the error can be better than the one obtained with I-PCE, with some other sample sets, it is the opposite: this questions confidence in NI-PCE, even when identified with a large number of samples.

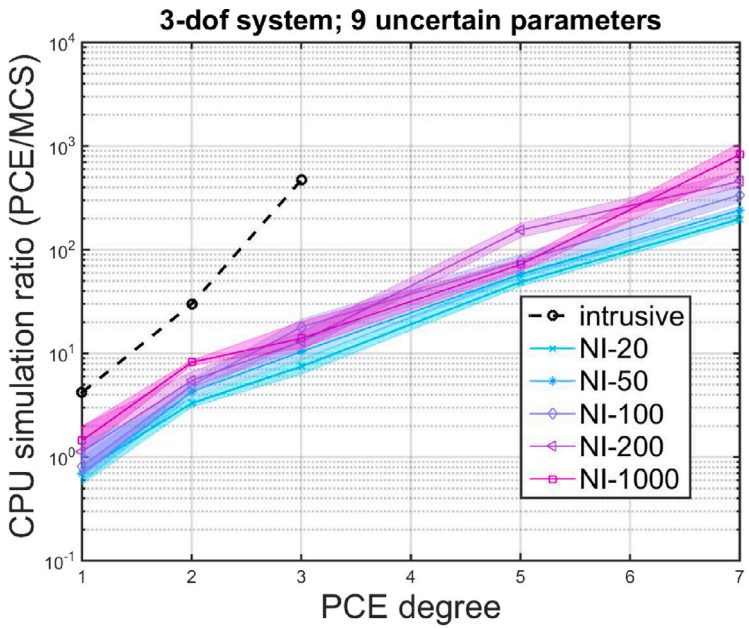

Fig. 5. 3-dof system with 9 random parameters: CPU simulation time comparison.

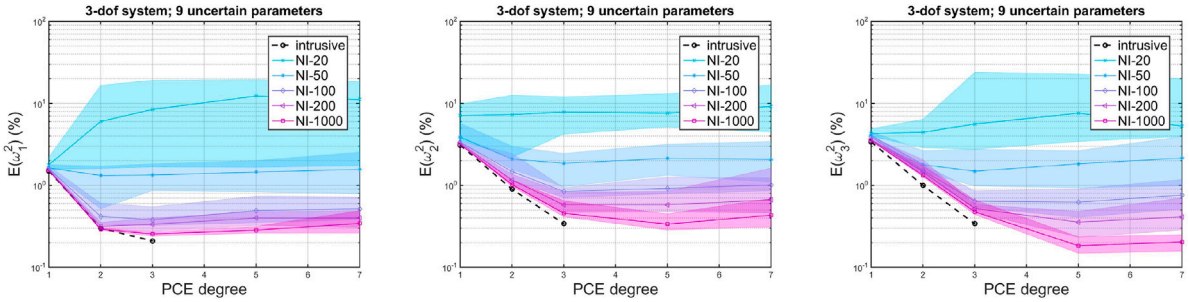

Fig. 6. 3-dof system with 9 random parameters: $\mathcal{E}_{\omega^2}$ comparison - dashed black line: I-PCE; solid coloured lines with markers: mean of NI-PCE errors; coloured area: envelope of NI-PCE errors.

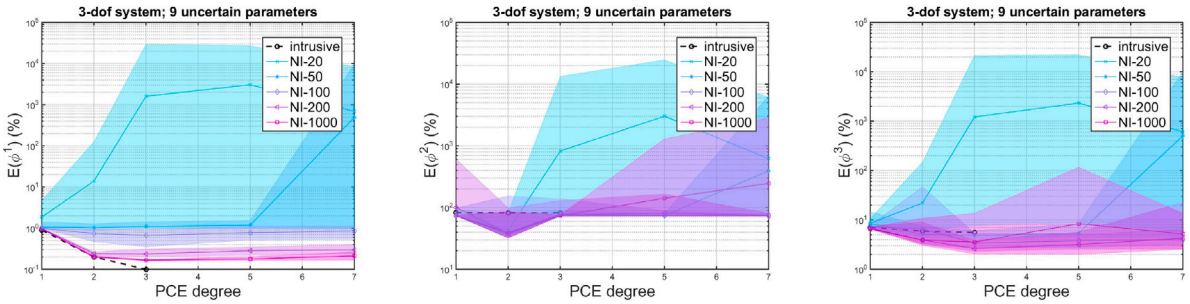

Fig. 7. 3-dof system with 9 random parameters: $\mathcal{E}_{\phi}$ comparison.

Considering the eigenvectors, the results shown in Fig. 7 are quite surprising: they strongly depend on the mode number. In particular, the lowest values of $\mathcal{E}_{\phi_i}$ are not in the same order of magnitude: $\mathcal{E}_{\phi_2}$ is about 10 times the best value of $\mathcal{E}_{\phi_3}$ which in turn is about 10 times the best value of $\mathcal{E}_{\phi_1}$. This result does not depend on the PCE approach. For the first eigenvector, I-PCE gives the smallest error, which is not always the case for the other two eigenvectors. Regarding NI-PCE, for the second and third eigenvectors it seems that increasing N_{spl} does not improve the result. However for the first eigenvector, the coloured areas decrease when N_{spl} increase. It clearly appears that using N_{spl}=20 samples to identify NI-PCE gives a very large coloured area: in that case the choice of the sample set is particularly crucial.

A global error over all the eigenmodes is studied through the FRF error, $\mathcal{E}_{FRF}$. Considering $\mathcal{E}_{\phi_2}$ and $\mathcal{E}_{\phi_3}$, it was not expected a very low error. Fig. 8 shows that it is about 8%–10% for both the non intrusive and intrusive approaches, which is not so bad compared to the ϕ_2 error. The intrusive approach performs better than NI-PCE, and it is important to notice that the results does not improve much by increasing N_{spl} from 100 to 1000 as the corresponding coloured areas overlap. Once again, it seems that the optimal degree of the sparse NI-PCE equals 3.

The influence of the N_{spl} identifying samples is noticeable, for NI-PCE approach, as it can be seen in Figs. 6–7–8. Indeed, for almost all the errors, the coloured area bounds are not really close to the corresponding mean lines.

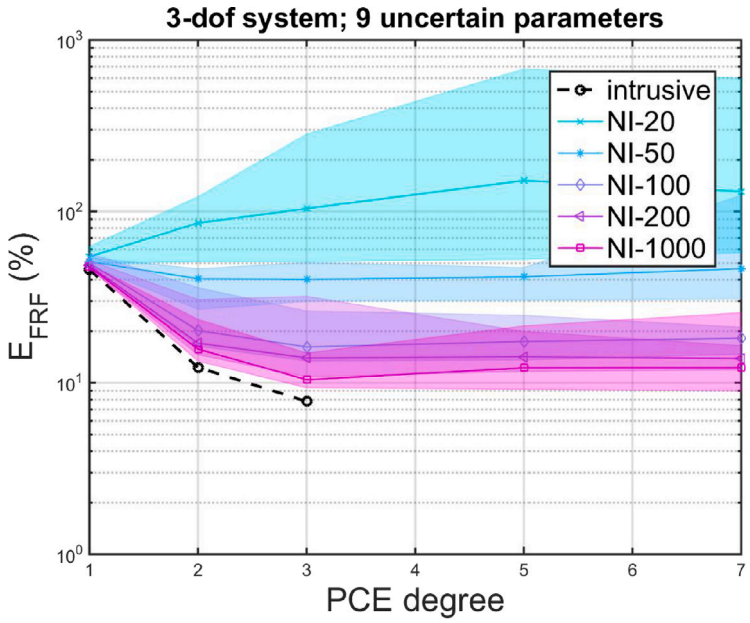

Fig. 8. 3-dof system with 9 random parameters: $\mathcal{E}_{FRF}$ comparison; the FRF is associated with dof 1.

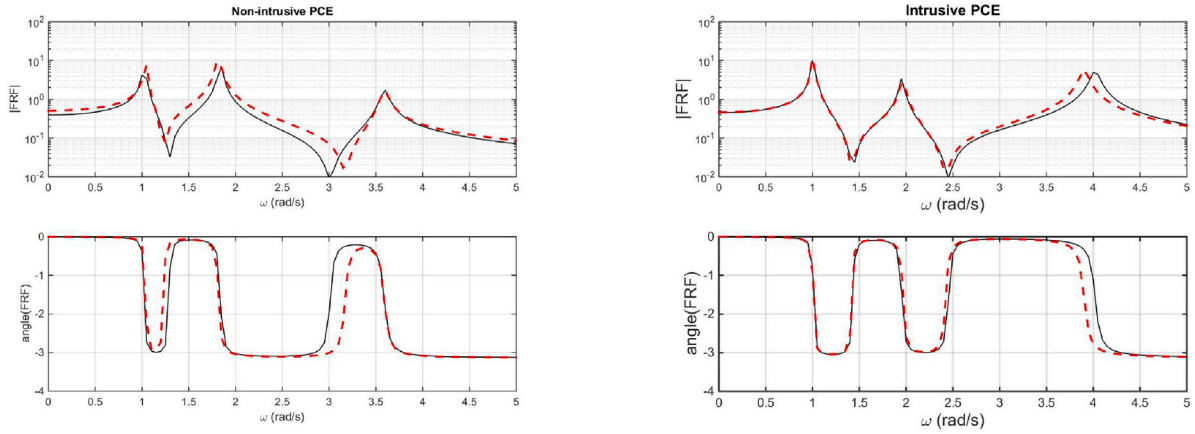

Fig. 9. Magnitude and argument of the FRF for the "worst sample" of the magnitude obtained from a direct simulation (MCS: black solid line) and the PCE of degree 3 (red dashed line); for NI-PCE, $N_{spl} = 200$.

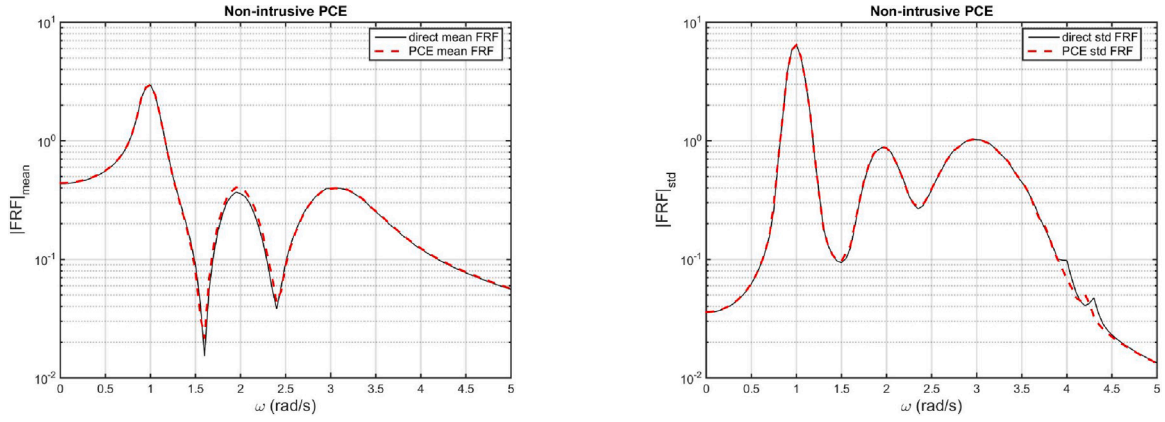

Fig. 10. Mean and standard deviation of the FRF from a direct simulation (MCS: black solid line) and NI-PCE of degree 3, $N_{spl} = 200$ (red dashed line).

It is always interesting to have a look on samples. That is why in Fig. 9, the "worst sample" of the FRF magnitude are plotted for both PCE approaches for a PCE degree equal to 3, and N_{spl} equal to 200. It appears that the intrusive approach is better than NI-PCE approach not only for the modulus of the FRF but also for the argument.

However, the mean and the standard deviation were always the same and similar to the ones obtained with the MCS approach, as shown on Fig. 10 for the non-intrusive case. For the intrusive approach, the mean and the standard deviation were also very close to the MCS ones.

7.3. Comparison of the two cases

The two cases are very different despite they are related to a very simple dynamical system. Indeed, in the first case the number of random parameters (r) is low, which means that the random space can be well described by a reasonably low number of samples: this is much more complicated for the second case with 9 random parameters.

The intrusive method requires to calculate expectation matrices: for the eigenproblem, the element number of such matrices can be as high as $r\times(P+1)^3$ where $(P+1)$, the number of terms in the PCE, depends on r and d, the PCE degree. Therefore, the method can be unaffordable when either r or d are quite large. This explains that the intrusive method is suitable for the first example. On the contrary, for the second example, r was quite high: using the intrusive method was limited to low PCE degree. The main drawback of I-PCE is that a specific program had to be written to find the expectations matrices and to solve Eq. (21). This takes time and the program is not optimized.

The main feature of NI-PCE is that a (sparse) PCE can be quite easily identified, as mentioned in Section 6 from available data. In both examples a quite low optimal PCE degree was identified: this illustrates that the quality of the results does not depend much on the PCE degree. Therefore, the non-intrusive method mainly relies on the capacity of the identification sample set to describe the random space, that is on the quality of the samples. This explains why increasing the number of identification samples increases the confidence in the identified PCE. That is why the usual process to find the optimal NI-PCE is adaptative: it consists in increasing the PCE degree and the number of samples progressively up to meet a criterion. The main interest of NI-PCE is that no new specific program has to be written as it is data-driven. However, it requires to run a model several times: the main limitation is the computational budget. Indeed, if one run takes several hours like in car crash simulations, the number of samples cannot be very high. In particular, in this case it is not possible to use several sample sets as done in this paper to study the confidence in the results. In the second example presented in the paper, NI-PCE is interesting because solving the eigenproblem of a 3-dof dynamical system is very quick: a wide range of data can be obtained. Nevertheless, the accuracy was not really better than the one obtain with the intrusive method even for a large number of samples: in particular, the variation of the results may quite large. This is due to the difficulty to explore a multidimensional random space.

An interesting critique and comparison between intrusive and non-intrusive can be found in [26].

8. Conclusions

This study presented a systematic comparison between intrusive and non-intrusive Polynomial Chaos Expansion (PCE) approaches for computing random eigenmodes in dynamical systems. Through detailed mathematical analysis and numerical experiments on a three-degree-of-freedom system with varying uncertainty parameters, the investigation revealed fundamental differences in implementation complexity, computational efficiency, and accuracy between the two approaches. The comparison encompassed both theoretical foundations and practical implementations, with particular attention to computational costs, accuracy thresholds, and scalability characteristics across different problem dimensions.

The research has established several novel contributions to the field of uncertainty quantification in structural dynamics:

1. First comprehensive quantitative comparison of intrusive and non-intrusive PCE methods for random eigenmode computation, revealing that intrusive PCE achieves superior accuracy with lower computational cost for low-dimensional problems, while non-intrusive PCE demonstrates better scalability for higher-dimensional systems.
2. Development of clear selection criteria for PCE implementation strategies based on problem dimensionality, required accuracy, and computational resources.
3. Discovery of previously undocumented relationships between sample size requirements and PCE degree in non-intrusive approaches, providing practical guidelines for implementation.

These findings have significant implications for both theoretical research and practical applications in structural dynamics and uncertainty quantification. The established criteria for selecting between intrusive and non-intrusive approaches will enable more efficient analysis of complex dynamical systems across various engineering disciplines. Furthermore, the discovered relationship between sample size and PCE degree offers practical guidelines for implementing non-intrusive PCE methods. Future research directions should focus on extending these comparisons to nonlinear systems, developing hybrid approaches that combine the advantages of both methods, and establishing theoretical bounds for the accuracy-efficiency trade-offs identified in this study.

CRediT authorship contribution statement

Eric Jacquelin: Writing – original draft, Validation, Software, Methodology, Investigation, Conceptualization. **Sondipon Adhikari:** Writing – review & editing, Validation, Supervision, Conceptualization. **Denis Brizard:** Writing – review & editing, Validation, Supervision.

Declaration of competing interest

The authors declare the following financial interests/personal relationships which may be considered as potential competing interests: Co-author Prof. Sondipon ADHIKARI is part of the editorial board of Probabilistic Engineering Mechanics If there are other authors, they declare that they have no known competing financial interests or personal relationships that could have appeared to influence the work reported in this paper.

Acknowledgment

The authors would like to thank one of the reviewers who drew their attention to the fact that the LARS method can automatically detect the OLS solution for the first example.

Appendix A. I-PC equations of mode k

First, Eq. (21) is projected on each PC $\Psi_m(\Xi)$ (m from 0 to P):

$$\forall m \in \{0,\dots,P\} \quad \sum_{i=0}^{r} < \xi_i m > \mathbf{K}_i \boldsymbol{\phi}^k + \sum_{i=0}^{r}\sum_{\substack{n=1\\ n\neq k}}^{N}\sum_{p=0}^{P}\langle \xi_i pm\rangle\ Y_{pn}^k\ \mathbf{K}_i\boldsymbol{\phi}^n - \omega_k^2 \sum_{i=0}^{r}\sum_{p=0}^{P}\langle \xi_i pm\rangle\ a_p^k\ \mathbf{M}_i\boldsymbol{\phi}^k - \omega_k^2 \sum_{i=0}^{r}\sum_{\substack{n=1\\ n\neq k}}^{N}\sum_{p=0}^{P}\sum_{q=0}^{P}\langle \xi_i pqm\rangle\ a_p^k\ Y_{qn}^k\ \mathbf{M}_i\boldsymbol{\phi}^n = 0 \qquad \text{(A.1)}$$

Second, Eq. (A.1) is projected on each deterministic eigenvector $\boldsymbol{\phi}^l$ (l from 1 to N):

$$\forall l \in \{1,\dots,N\}, \quad \forall m \in \{0,\dots,P\}$$

$$\sum_{i=0}^{r}\sum_{\substack{n=1\\n\neq k}}^{N}\sum_{p=0}^{P}\langle\xi_i pm\rangle\ Y_{pn}^{k}\ {}^{T}\boldsymbol{\phi}^{l}\mathbf{K}_i\boldsymbol{\phi}^{n}$$
$$-\omega_k^2\sum_{i=0}^{r}\sum_{p=0}^{P}\langle\xi_i pm\rangle\ a_p^k\ {}^{T}\boldsymbol{\phi}^{l}\mathbf{M}_i\boldsymbol{\phi}^{k}$$
$$-\omega_k^2\sum_{i=0}^{r}\sum_{\substack{n=1\\n\neq k}}^{N}\sum_{p=0}^{P}\sum_{q=0}^{P}\langle\xi_i pqm\rangle\ a_p^k\ Y_{qn}^{k}\ {}^{T}\boldsymbol{\phi}^{l}\mathbf{M}_i\boldsymbol{\phi}^{n}=-\sum_{i=0}^{r}\langle\xi_i m\rangle\ {}^{T}\boldsymbol{\phi}^{l}\mathbf{K}_i\boldsymbol{\phi}^{k}\quad(A.2)$$

New matrices are defined, $\forall i\in\{0,\dots,r\}$, $\forall m\in\{0,\dots,P\}$, $\forall l\in\{1,\dots,N\}$:

$$\begin{aligned}
\mathbf{a}^k &= {}^{T}[a_0^k\ \cdots\ a_P^k]\in\mathbf{R}^{(P+1)\times 1}\\
\forall n\in\{1,\dots,N\}\backslash\{k\},\quad \mathbf{Y}_n^k &= {}^{T}[Y_{0n}^k\ \cdots\ Y_{Pn}^k]\in\mathbf{R}^{(P+1)\times 1}\\
\forall n\in\{1,\dots,N\}\backslash\{k\},\quad \mathbf{Y}^k &= {}^{T}[{}^{T}\mathbf{Y}_1^k\ \cdots\ {}^{T}\mathbf{Y}_{n\neq k}^k\\
&\quad\cdots\ {}^{T}\mathbf{Y}_N^k]\in\mathbf{R}^{(P+1)(N-1)\times 1}\\
\mathbf{K}^i=[\mathbf{K}_{ln}^i]\in\mathbf{R}^{N\times N}\ &\text{with}\ \mathbf{K}_{ln}^i={}^{T}\boldsymbol{\phi}^{l}\mathbf{K}_i\boldsymbol{\phi}^{n}\\
\mathbf{M}^i=[\mathbf{M}_{ln}^i]\in\mathbf{R}^{N\times N}\ &\text{with}\ \mathbf{M}_{ln}^i={}^{T}\boldsymbol{\phi}^{l}\mathbf{M}_i\boldsymbol{\phi}^{n}\\
\mathbf{M3}^i=[\mathbf{M3}_{mp}^i]\in\mathbf{R}^{(P+1)\times(P+1)}\ &\text{with}\ \mathbf{M3}_{mp}^i=\langle\xi_i pm\rangle\\
\mathbf{M4}^{im}=[\mathbf{M4}_{pq}^{im}]\in\mathbf{R}^{(P+1)\times(P+1)}\ &\text{with}\ \mathbf{M4}_{pq}^{im}=\langle\xi_i pqm\rangle\\
\mathbf{MM4}^{lm}=[\mathbf{MM4}_1^{lm}\cdots\mathbf{MM4}_{n\neq k}^{lm}\cdots\mathbf{MM4}_N^{lm}]\ &\text{with}\ \mathbf{MM4}_n^{lm}\\
=\sum_{i=0}^{r}\mathbf{M}_{ln}^i\ \mathbf{M4}^{im}&\in\mathbf{R}^{(P+1)\times(P+1)}\\
\mathbf{f}^l(\mathbf{a}^k,\mathbf{Y}^k)=[\mathbf{f}_m^l(\mathbf{a}^k,\mathbf{Y}^k)]\in\mathbf{R}^{(P+1)\times 1}\ &\text{with}\ \mathbf{f}_m^l(\mathbf{a}^k,\mathbf{Y}^k)\\
&={}^{T}\mathbf{a}^k\ \mathbf{MM4}^{lm}\ \mathbf{Y}^k
\end{aligned}$$

$$\mathbf{B}^{lk}=\frac{1}{C_1}\begin{bmatrix}C_1\mathbf{K}_{lk}^0\\ \mathbf{K}_{lk}^1\\ \vdots\\ \mathbf{K}_{lk}^r\\ 0\\ \vdots\\ 0\end{bmatrix}\in\mathbf{R}^{(P+1)}\ \text{because}\ \forall i\geq 1,\langle\xi_i m\rangle$$
$$=\frac{\delta_{i,m}}{C_1}\ \text{and}\ C_1\text{: }\xi_i\ \text{coefficient of}\ \psi_1(\xi_i)$$

Therefore, Eq. (A.2) is, $\forall\ l=1,\dots,N$:

$$\sum_{\substack{n=1\\n\neq k}}^{N}\left(\sum_{i=0}^{r}\mathbf{K}_{ln}^i\ \mathbf{M3}^i\right)\mathbf{Y}_n^k\ -\ \omega_k^2\left(\sum_{i=0}^{r}\mathbf{M}_{lk}^i\ \mathbf{M3}^i\right)\mathbf{a}^k\ -\omega_k^2\ \mathbf{f}^l(\mathbf{a}^k,\mathbf{Y}^k)=-\ \mathbf{B}^{lk}\quad(A.3)$$

Additional matrices are introduced:

$$\forall n\in\{1,\dots,N\}\backslash\{k\},\ \mathbf{KM3}^{ln}=\sum_{i=0}^{r}\mathbf{K}_{ln}^i\ \mathbf{M3}^i\ \in\mathbf{R}^{(P+1)\times(P+1)}$$
$$\mathbf{MM3}^{lk}=\sum_{i=0}^{r}\mathbf{M}_{lk}^i\ \mathbf{M3}^i\ \in\mathbf{R}^{(P+1)\times(P+1)}$$

Eq. (A.3) is now:

$$\forall l\in\{1,\dots,N\}\quad\sum_{\substack{n=1\\n\neq k}}^{N}\mathbf{KM3}^{ln}\ \mathbf{Y}_n^k\ -\ \omega_k^2\ \mathbf{MM3}^{lk}\ \mathbf{a}^k\ -\ \omega_k^2\ \mathbf{f}^l(\mathbf{a}^k,\mathbf{Y}^k)=-\mathbf{B}^{lk}\quad(A.4)$$

Or, alternatively,

$$\begin{bmatrix}\mathbf{KM3}^{11} & \cdots & \mathbf{KM3}^{1N} & -\omega_k^2\mathbf{MM3}^{1k}\\ \vdots & \mathbf{KM3}^{ln\neq k} & \vdots & \vdots\\ \mathbf{KM3}^{N1} & \cdots & \mathbf{KM3}^{NN} & -\omega_k^2\mathbf{MM3}^{Nk}\end{bmatrix}\begin{bmatrix}\mathbf{Y}_1^k\\ \vdots\\ \mathbf{Y}_N^k\\ \mathbf{a}^k\end{bmatrix}$$
$$-\ \omega_k^2\begin{bmatrix}\mathbf{f}^1(\mathbf{a}^k,\mathbf{Y}^k)\\ \vdots\\ \mathbf{f}^N(\mathbf{a}^k,\mathbf{Y}^k)\end{bmatrix}=-\begin{bmatrix}\mathbf{B}^{1k}\\ \vdots\\ \mathbf{B}^{Nk}\end{bmatrix}\quad(A.5)$$

Appendix B. Expectation matrices $\mathbf{M3}^i$, $\mathbf{M4}^{im}$

Eq. (5) gives the definition of PC:

$$\Psi_p(\Xi)=\Psi_J(\Xi)=\prod_{i=1}^{r}\psi_{J_i}(\xi_i)\quad(B.1)$$

where J is the multi-index corresponding to single-index p, as explained in Section 3.

In the following $\psi_{J_i}(\xi_i)$ is supposed to be either a Hermite polynomial or a Legendre polynomial; they are also supposed to be orthonormal. They follow the recurrence relation (28), which may be rewritten as:

$$\forall J_i>0,\quad \xi_i\ \psi_{J_i}(\xi_i)\ =\ A_{J_i}\ \psi_{J_i+1}(\xi_i)-B_{J_i}\ \psi_{J_i}(\xi_i)+C_{J_i}\psi_{J_i-1}(\xi_i)\quad(B.2)$$

B.1. Expectation matrix $\mathbf{M3}^i$

It is required to calculate

$$\forall i\in\{1,\dots,r\}\ \text{and}\ \forall p,q\in\{0,\dots,P\}\quad\langle\xi_i\ p\ q\rangle\ =\ \langle\xi_i\ \Psi_J(\Xi)\ \Psi_{J'}(\Xi)\rangle\quad(B.3)$$

From Eq. (B.1)

$$\langle\xi_i\ \Psi_J(\Xi)\ \Psi_{J'}(\Xi)\rangle=\left(\prod_{\substack{\alpha=1\\\alpha\neq i}}^{r}\langle\psi_{J_\alpha}(\xi_\alpha)\ \psi_{J'_\alpha}(\xi_\alpha)\rangle\right)\langle\xi_i\ \psi_{J_i}(\xi_i)\ \psi_{J'_i}(\xi_i)\rangle\quad(B.4)$$

The polynomials are orthonormal

$$\prod_{\substack{\alpha=1\\\alpha\neq i}}^{r}\langle\psi_{J_\alpha}(\xi_\alpha)\ \psi_{J'_\alpha}(\xi_\alpha)\rangle=\prod_{\substack{\alpha=1\\\alpha\neq i}}^{r}\delta_{J_\alpha J'_\alpha}\quad(B.5)$$

where δ is the Kronecker symbol.

From Eq. (B.2), $\forall J_i>0$

$$\begin{aligned}\langle\xi_i\ \psi_{J_i}(\xi_i)\ \psi_{J'_i}(\xi_i)\rangle\ &=\ A_{J_i}\langle\psi_{J_i+1}(\xi_i)\ \psi_{J'_i}(\xi_i)\rangle-B_{J_i}\langle\psi_{J_i}(\xi_i)\ \psi_{J'_i}(\xi_i)\rangle\\ &\quad+C_{J_i}\langle\psi_{J_i-1}(\xi_i)\ \psi_{J'_i}(\xi_i)\rangle\\ &=\ A_{J_i}\delta_{J_i+1\,J'_i}-B_{J_i}\delta_{J_i\,J'_i}+C_{J_i}\delta_{J_i-1\,J'_i}\end{aligned}\quad(B.6)$$

Each element of matrix $\mathbf{M3}^i$ has an analytic expression:

$$\mathbf{M3}_{pq}^i\ =\ \langle\xi_i\ p\ q\rangle\ =\ \left(\prod_{\substack{\alpha=1\\\alpha\neq i}}^{r}\delta_{J_\alpha J'_\alpha}\right)\times\left(A_{J_i}\delta_{J_i+1\,J'_i}-B_{J_i}\delta_{J_i\,J'_i}+C_{J_i}\delta_{J_i-1\,J'_i}\right)\quad(B.7)$$

Coefficients A_{J_i}, B_{J_i} and C_{J_i} can be found in Table C.2.

B.2. Expectation matrix $\mathbf{M4}^{im}$

It is required to calculate for all $i\in\{1,\dots,r\}$ and for all $m,p,q\in\{0,\dots,P\}$

$$\begin{aligned}\langle\xi_i\ m\ p\ q\rangle\ &=\ \langle\xi_i\ \Psi_M(\Xi)\Psi_J(\Xi)\ \Psi_{J'}(\Xi)\rangle\\ &=\left(\prod_{\substack{\alpha=1\\\alpha\neq i}}^{r}\langle\psi_{M_\alpha}(\xi_\alpha)\ \psi_{J_\alpha}(\xi_\alpha)\ \psi_{J'_\alpha}(\xi_\alpha)\rangle\right)\langle\xi_i\ \psi_{M_i}(\xi_i)\ \psi_{J_i}(\xi_i)\ \psi_{J'_i}(\xi_i)\rangle\end{aligned}\quad(B.8)$$

From Eq. (B.2)

$$\begin{aligned}\forall M_i>0,\quad\langle\xi_i\ \psi_{M_i}(\xi_i)\ \psi_{J_i}(\xi_i)\ \psi_{J'_i}(\xi_i)\rangle\ &=\ A_{M_i}\langle\psi_{M_i+1}(\xi_i)\ \psi_{J_i}(\xi_i)\ \psi_{J'_i}(\xi_i)\rangle\\ &\quad-B_{M_i}\langle\psi_{M_i}(\xi_i)\ \psi_{J_i}(\xi_i)\ \psi_{J'_i}(\xi_i)\rangle\\ &\quad+C_{M_i}\langle\psi_{M_i-1}(\xi_i)\ \psi_{J_i}(\xi_i)\ \psi_{J'_i}(\xi_i)\rangle\end{aligned}\quad(B.9)$$

Table C.2
Information on normalized Hermite and Legendre polynomial.

$P_i(x)$	Normalized Hermite $h_i(x)$	Normalized Legendre $l_i(x)$
Domain D	$]-\infty,\ +\infty\ [$	$[-1,\ +1]$
Density of the measure $p_x(x)$	$\frac{\exp(-x^2/2)}{\sqrt{2\pi}}$	$\frac{1}{2}$
$P_0(x)$	$h_0(x)=1$	$l_0(x)=1$
$P_1(x)$	$h_1(x)=x$	$l_1(x)=\sqrt{3}\ x$
C_1	1	$\sqrt{3}$
A_i	$\sqrt{i+1}$	$\frac{i+1}{\sqrt{(2i+1)\times(2i+3)}}$
B_i	0	0
C_i	$\sqrt{i}$	$\frac{i}{\sqrt{(2i-1)\times(2i+1)}}$
recurrence equation	$x\ P_i(x) = A_i\ P_{i+1}(x) + C_i\ P_{i-1}(x)$ $P_{i+1}(x) = \frac{1}{A_i} x\ P_i(x) - \frac{C_i}{A_i} P_{i-1}(x)$	

From Eqs. (B.8)–(B.9), it is clear that calculating $\langle \xi_i\ m\ p\ q\rangle$ reduces to calculating $\langle \psi_i(\xi)\ \psi_j(\xi)\ \psi_l(\xi)\rangle$. It turns out that an analytic expression exists for Hermite polynomial [27], and for Legendre polynomial [28].

Orthonormal Hermite polynomial [27] (p. 390, ex. 87)

$$\text{if } s\in\mathbf{N},\quad \langle i,j,l\rangle = \frac{\sqrt{i!\ j!\ l!}}{(s-i)!\ (s-j)!\ (s-l)!}\ \mathrm{Ind}_{\max(i,j,l)}(s) \tag{B.10}$$

$$\text{if } s\notin\mathbf{N},\quad \langle i,j,l\rangle = 0 \tag{B.11}$$

with

- $s=(i+j+l)/2$,
- function $\mathrm{Ind}_m(s)$ is equal to unity if $0\le m\le s$ and to zero otherwise.

Orthonormal Legendre polynomial [28]

$$\langle i,j,l\rangle = \frac{\sqrt{(2i+1)(2j+1)(2l+1)}}{2s+1}\ \frac{\mathcal{A}(s-i)\mathcal{A}(s-j)\mathcal{A}(s-l)}{\mathcal{A}(s)} \tag{B.12}$$

with

- $s=(i+j+l)/2$,
- $\mathcal{A}(s)$:

$$\text{if } s\in\mathbf{N},\quad \mathcal{A}(s)=\frac{1\times3\times5\times\cdots\times(2s-1)}{s!}=\frac{(2s)!}{2^s(s!)^2} \tag{B.13}$$

$$\text{if } s\notin\mathbf{N},\quad \mathcal{A}(s)=0 \tag{B.14}$$

$$\text{if } s<0,\quad \mathcal{A}(s)=0 \tag{B.15}$$

Note that in [28], the following expression is given

$$\int_{-1}^{1} L_i(x)\ L_j(x)\ L_l(x)\ \mathrm{d}x = \frac{2}{2s+1}\ \frac{\mathcal{A}(s-i)\mathcal{A}(s-j)\mathcal{A}(s-l)}{\mathcal{A}(s)} \tag{B.16}$$

Eq. (B.16) is transformed into Eq. (B.12) by taking into account that

- normalized Legendre polynomials are used: $l_i(x)=\sqrt{2i+1}\ L_i(x)$
- $\langle i,j,l\rangle = \int_{-1}^{1} l_i(x)\ l_j(x)\ l_l(x)\ p_x(x)\ \mathrm{d}x$ with $p_x(x)=1/2$; factor $p_x(x)$ is omitted in (B.16)

Appendix C. Information on Hermite and Legendre polynomial families

Information required to obtain all the expectations matrices are given in Table C.2 for normalized Hermite and Legendre polynomials.

Data availability

The link to the original codes is shared in the attach file step

Random Modes (Original data) (Github)

References

[1] P. Benner, A. Onwunta, S. Stoll, A low-rank inexact Newton–Krylov method for stochastic Eigenvalue problems, Comput. Methods Appl. Math. 19 (1) (2019) 5–22.
[2] H. Hakula, V. Kaarnioja, M. Laaksonen, Approximate methods for stochastic eigenvalue problems, Appl. Math. Comput. 267 (2015) 664–681.
[3] H. Hakula, M. Laaksonen, Asymptotic convergence of spectral inverse iterations for stochastic Eigenvalue problems, Internat. J. Numer. Methods Engrg. 142 (3) (2019) 577–609.
[4] O. Dessombz, A. Diniz, F. Thouverez, L. Jézéquel, Analysis of stochastic structures: Pertubation method and projection on homogeneous chaos, in: 7th International Modal Analysis Conference IMAC-SEM, Kissimmee, Floride-USA, 1999.
[5] B. Van Den Nieuwenhof, J.P. Coyette, Modal approaches for the stochastic finite element analysis of structures with material and geometric uncertainties, Comput. Methods Appl. Mech. Engrg. 192 (33–34) (2003) 3705–3729.
[6] L. Pichler, H.J. Pradlwarter, G.I. Schuëller, A mode-based meta-model for the frequency response functions of uncertain structural systems, Comput. Struct. 87 (5–6) (2009) 332–341.
[7] D. Ghosh, Application of the random eigenvalue problem in forced response analysis of a linear stochastic structure, Arch. Appl. Mech. 83 (9) (2013) 1341–1357.
[8] E. Pagnacco, E. Souza de Cursi, R. Sampaio, Subspace inverse power method and polynomial chaos representation for the modal frequency responses of random mechanical systems, Comput. Mech. 58 (2016) 129–149.
[9] E. Jacquelin, O. Dessombz, J.J. Sinou, S. Adhikari, M.I. Friswell, Polynomial chaos-based extended Padé expansion in structural dynamics, Int. J. Numer. Methods Eng. 111 (12) (2017) 1170–1191.
[10] S. Adhikari, S. Chakraborty, Random matrix Eigenvalue problems in structural dynamics: An iterative approach, Mech. Syst. Signal Process. 164 (1) (2022).
[11] H. Zhang, Y. Liu, B. Huang, X. Wu, Z. Wu, M.H. Faber, Dynamic characteristics of vertically irregular structures with random fields of different probability distributions based on stochastic homotopy method, Mech. Syst. Signal Process. 220 (2024) 111638.
[12] E. Jacquelin, D. Brizard, S. Adhikari, M.I. Friswell, Time-domain response of damped stochastic multiple-degree-of-freedom systems, J. Eng. Mech. 146 (1) (2020) 06019005.
[13] R.G. Ghanem, P.D. Spanos, Stochastic Finite Elements: A Spectral Approach, Springer-Verlag, New York, USA, 1991.
[14] N. Wiener, The homogeneous chaos, Am. J. Math. 60 (1938) 897–936.
[15] R.G. Ghanem, D. Ghosh, Efficient characterization of the random eigenvalue problem in a polynomial chaos decomposition, Internat. J. Numer. Methods Engrg. 72 (2007) 486–504.
[16] B. Pascual, S. Adhikari, Hybrid perturbation-polynomial chaos approaches to the random algebraic eigenvalue problem, Comput. Methods Appl. Mechacnics Eng. 217–220 (2012) 153–167.
[17] D. Ghosh, R.G. Ghanem, An invariant subspace-based approach to the random eigenvalue problem of systems with clustered spectrum, Internat. J. Numer. Methods Engrg. 91 (4) (2012) 378–396.

[18] Z. Zheng, M. Beer, U. Nackenhorst, An efficient reduced-order method for stochastic eigenvalue analysis, Internat. J. Numer. Methods Engrg. 123 (23) (2022) 5884–5906.
[19] M. Berveiller, B. Sudret, M. Lemaire, Stochastic finite elements: a non intrusive approach by regression, Eur. J. Comput. Mech. 15 (1–3) (2006) 81–92.
[20] G. Onorato, G.J.A. Loeven, G. Ghorbaniasl, H. Bijl, C. Lacor, Comparison of intrusive and non-intrusive polynomial chaos method for CFD applications in aeronautics, in: V European Conference on Computational Fluid Dynamics, Lisbon, Portugal, 2010.
[21] D. Xiu, Numerical Methods for Stochastic Computations – A Spectral Method Approach, Princeton University Press, 2010.
[22] O. Dessombz, Analyse dynamique de structures comportant des paramètres incertains (Ph.D. thesis), École Centrale de Lyon, 2000.
[23] G. Blatman, B. Sudret, An adaptive algorithm to build up sparse polynomial chaos expansions for stochastic finite element analysis, Probabilistic Eng. Mech. 25 (2) (2010) 183–197.
[24] G. Blatman, B. Sudret, Adaptive sparse polynomial chaos expansion based on least angle regression, J. Comput. Phys. 230 (6) (2011) 2345–2367.
[25] B. Bhattacharyya, E. Jacquelin, D. Brizard, Stochastic analysis of a crash box under impact loading by an adaptive POD-PCE model, Struct. Multidiscip. Optim. 65 (8) (2022).
[26] A. O'Hagan, Polynomial chaos: A tutorial and critique from a statistician's perspective, SIAM/ ASA J. Uncertain. Quantif. 20 (2013) 1–20.
[27] G. Szegö, Orthogonal polynomials, fourth ed., Colloquium Publications, vol. 23, American Mathematical Society, Providence, Rhode Island, 1975.
[28] J.C. Adams, On the expression of the product of any two Legendre's coefficients by means of a series of Legendre's coefficients, Proc. R. Soc. Lond 27 (185–189) (1878) 63–71.